for the bromite–iodide reaction, since eq 1, which consumes H^+, will be further retarded by the much higher pH of the bromite system. The lack of stirring rate sensitivity in the batch bromite–iodide system is consistent with this view, since in the batch configuration it is not necessary for spatially separated feedstreams to mix. Menzinger and Dutt[11] also report spatial synchronization in the chlorite–iodide flow system, consistent with our observations in the bromite–iodide reaction.

In view of the many chlorite-based oscillators[21] that have been discovered in the past decade, one may wonder whether there are large numbers of bromite-based oscillating reactions waiting to be uncovered. The answer may depend upon how the oscillations in the present system actually arise, i.e., on the mechanism. It seems quite likely that one can construct oscillators analogous to the chlorite–iodide–oxidant systems[21b] by adding appropriate oxidizing agents to the present system. Such oscillators might be expected to be more robust, less sensitive to stirring, and perhaps even show batch oscillation.[21c] If, however, the existence of a stable bromine(IV) species is essential, as ClO_2 apparently is in the chlorite–iodide–malonic acid batch oscillator,[22] then the lower stability of BrO_2 may prevent observation of oscillatory behavior in the analogous bromite systems. Whether one can replace iodide ion with other species as has been done, for example, with several sulfur compounds in chlorite oscillators,[21d,e] may depend upon whether oscillation in the bromite system is attributable more to the autocatalytic effect of I_2 or to the inhibitory effect of I^-. The former effect will be much easier to duplicate with other reagents than will the latter. In any case, the search for new bromite oscillators should lead to a deeper understanding of the chemistry of this fascinating species.

Acknowledgment. We thank Kenneth Kustin and Roberto Faria for helpful discussions. This work was supported by the National Science Foundation (CHE-9023294), by the Hungarian Academy of Sciences (OTKA 1/3 No. 2275), and by a U.S.-Hungarian cooperative grant from the NSF and the Hungarian Academy.

---

(21) (a) Orbán, M.; De Kepper, P.; Epstein, I. R.; Kustin, K. *Nature* **1981**, *292*, 816. (b) Orbán, M.; Dateo, C.; De Kepper, P.; Epstein, I. R. *J. Am. Chem. Soc.* **1982**, *104*, 5911. (c) De Kepper, P.; Epstein, I. R.; Orbán, M.; Kustin, K. *J. Phys. Chem.* **1982**, *86*, 170. (d) Orbán, M.; De Kepper, P.; Epstein, I. R. *J. Phys. Chem.* **1982**, *86*, 431. (e) Alamgir, M.; Epstein, I. R. *Int. J. Chem. Kinet.* **1985**, *17*, 429.

(22) Lengyel, I.; Rábai, Gy.; Epstein, I. R. *J. Am. Chem. Soc.* **1990**, *112*, 4606.

Photochemistry of Binuclear Ferraazetines: CO vs Alkyne Insertion

Chad A. Mirkin,[†,‡] Timothy J. Oyer,[†] Mark S. Wrighton,[*,†] Thomas E. Snead,[§] and Gregory L. Geoffroy[§]

Contribution from the Departments of Chemistry, Massachusetts Institute of Technology, Cambridge, Massachusetts 02139, and The Pennsylvania State University, University Park, Pennsylvania 16802. *Received June 3, 1991. Revised Manuscript Received September 16, 1991*

Abstract: An investigation of the low-temperature matrix isolation photochemistry of ferraazetines, $Fe_2(\mu\text{-CRCHNBu}^t)(CO)_6$ (**1a**, R = H; **1b**, R = CH=CHPh) in rigid matrices is reported. Near-UV irradiation of **1a** and **1b** in CO-saturated methylcyclohexane (MCH) at 298 K yields ferrapyrrolinones **2a** and **2b**, $Fe_2\{\mu\text{-CRCHNBu}^t\text{C(O)}\}(CO)_6$, and in the presence of *tert*-butylacetylene, **1a** and **1b** form ferrapyridines **3a** and **3b**, $Fe_2(\mu\text{-Bu}^t\text{CCHCRCH=NBu}^t)(CO)_6$. The photoinduced insertion of CO and *tert*-butylacetylene occur at different positions in the ferraazetine metallacycle. CO insertion occurs between the Fe–N bond of the metallacycle whereas *tert*-butylacetylene insertion occurs between the Fe–C bond. At 15 or 8 K in MCH, 1:1 *tert*-butyl acetylene/MCH, or CO matrices, the primary photoprocess for **1a** and **1b** involves Fe–N bond cleavage to yield coordinatively unsaturated compounds **4a** and **4b**, respectively. Irradiation of **4a** in a MCH matrix gives bridging CO compound **5**, $Fe_2(\mu\text{-CHCHNBu}^t)(\mu\text{-CO})(CO)_5$, which is formed by a CO ligand swinging from the adjacent Fe center to occupy the vacant coordination site created by the Fe–N cleavage. In a 1:1 *tert*-butylacetylene/MCH matrix, irradiation of **4a** at 98 K gives a *tert*-butylacetylene adduct **6**, $Fe_2(\mu\text{-CHCHNBu}^t)(CO)_6(\text{Bu}^t\text{C}\equiv\text{CH})$. When warmed to 298 K, **6** inerts the *tert*-butylacetylene ligand to form **3a**. Irradiation of **4a** in a ^{13}CO matrix at 8 K gives CO insertion product **2a** with ^{13}CO incorporation at a terminal position with no evidence of incorporation at the carbonyl of the acyl ligand. When **4b** is irradiated in MCH at 15 K, compound **7**, $Fe_2\{\mu\text{-C(CH=NBu}^t\text{)CHCHPh}\}(CO)_6$, is formed. **7** derives from a ligand exchange of the $C{=}NBu^t$ group of the ferraazetine ring in **4b** for its pendant styryl group, CH=CHPh. When irradiated at 98 K or 298 K in MCH, **1b** forms **7** with no detectable intermediates and the photoconversion is much faster at these temperatures than at 15 K. At 298 K **7** quantitatively re-forms **1b** after 2 h in the dark.

Introduction

We report the low-temperature photochemistry of binuclear ferraazetines **1a** and **1b** with CO and *tert*-butylacetylene in solution and in rigid matrices at $T \leq 98$ K. It has been recently reported that the near-UV irradiation of **1a** at 298 K in the presence of CO (1 atm) produces ferrapyrrolinone **2** and in the presence of alkyne, **1a** forms ferrapyridine complex **3**, eqs 1 and 2.[1,2] The reaction between **1** and monosubstituted alkynes is general and quite regioselective with only one of two possible regioisomers being formed as product, eq 2. Compound **3** and its derivatives have proven useful in the development of a high-yield regioselective

---

[*] To whom correspondence should be addressed.

[†] Massachusetts Institute of Technology.

[‡] Present address: Department of Chemistry, Northwestern University, Evanston, IL 60208-3113.

[§] The Pennsylvania State University.

(1) (a) Mirkin, C. A.; Lu, K.; Snead, T. E.; Young, B. A.; Geoffroy, G. L.; Rheingold, A. L.; Haggerty, B. S. *J. Am. Chem. Soc.* **1991**, *113*, 3800. (b) Mirkin, C. A.; Lu, K.; Geoffroy, G. L.; Rheingold, A. L.; Staley, D. L. *J. Am. Chem. Soc.* **1989**, *18*, 7279.

(2) Mirkin, C. A.; Lu, K.; Snead, T. E.; Geoffroy, G. L.; Rheingold, A. L. *J. Am. Chem. Soc.* **1990**, *112*, 2809.

0002-7863/92/1514-1256$03.00/0

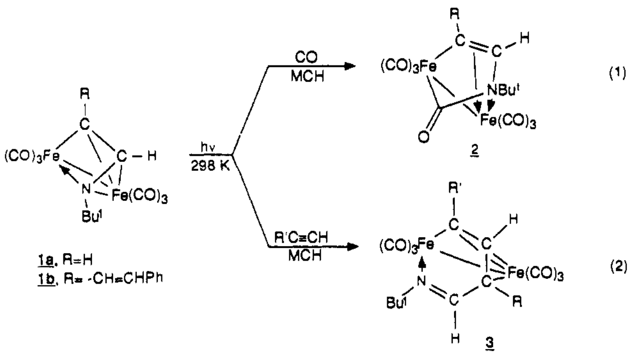

synthesis for 2-pyridinones, an important class of biologically active heterocycles.[2]

The most intriguing aspect of the two photochemically induced transformations illustrated in eqs 1 and 2 is the difference in the site of insertion for the substrates. CO insertion occurs between the Fe–N bond of the ferraazetine ring, eq 1, whereas alkyne insertion occurs between the Fe–C bond of the metallacycle, eq 2. At room temperature, no intermediates can be spectroscopically observed in the formation of either ferrapyrrolinone **2** or ferrapyridine **3**. The low-temperature matrix isolation photochemistry of **1a** and **1b** in methylcyclohexane (MCH), however, allows for the spectroscopic observation of intermediates along the pathway to formation of compounds **2** and **3**. Herein, we present the data from an FTIR investigation of the intermediates involved in the photochemistry of ferraazetines **1a** and **1b** to form compounds **2a,b** and **3a,b**. The mechanistic implications of the intermediates involved are also discussed.

Results

Photochemistry of *tert*-Butylferraazetine 1a at 98 K in a MCH Matrix. Near-UV irradiation of compound **1a** in a rigid MCH matrix at 98 K results in rapid conversion to a new species, **4a** (Figure 1A). Compound **4a** is also photosensitive and upon further irradiation proceeds to give **5** (Figure 1B). Dissociative loss of CO from **1a** is *not* a primary photoprocess as indicated by the absence of free CO in the matrix at 2132 cm^{-1}. The IR spectrum of **4a**, which exhibits terminal CO absorptions of 2072, 2027, 1996, and 1967 cm^{-1}, is very similar to that of **1a**, indicating that the coordination geometry around each metal center has not been significantly changed in the transformation of **1a** to **4a**. Note that the three carbonyl bands of **4a** (2072, 2027, 1996 cm^{-1}) are shifted to only slightly higher energy than those of **1a** (2069, 2025, 1992 cm^{-1}), quite possibly due to a slight decrease in electron density at one of the Fe centers. The shift for the three carbonyl bands in Figure 1A is similar in direction to that observed to accompany the photoextrusion of pyridine from $(CO)_5W(py)$.[3] Based on the lack of CO loss and the similarity of the CO region in the IR, we propose that **4a** is derived from **1a** by the light-induced extrusion of the N atom of the metallacycle from one of the $Fe(CO)_3$ centers to which it is coordinated (Figure 1A). At 98 K **4a** reverts slowly ($t_{1/2} > 30$ min) in the dark to **1a**.

Photolysis of **1a** at 98 K results in the eventual formation of **5** (Figure 1B). Based on the time dependence of IR spectral changes, **5** is a secondary photoproduct formed by the irradiation of **4a**. The most significant feature in the IR spectrum of **5** is a low-energy band at 1840 cm^{-1}, assigned to a bridging CO ligand (Figure 1B). In addition, there are terminal CO bands for **5** at 2068, 2005, 2003, 1988, and 1957 cm^{-1}. The proposed bridging CO of **5** is analogous to the bridging CO ligands of $Cp_2Fe_2(CO)_3$ formed by the light-induced CO loss from $Cp_2Fe_2(CO)_4$.[4] Furthermore, the band at 1840 cm^{-1} in the IR spectrum of **5** compares quite well to bands assigned to bridging carbonyl ligands for other group VIII organometallic complexes (e.g., $Fe_2(CO)_9$, 1828 cm^{-1}).[5] Compound **5**, unlike compound **4a**, is thermally inert at 98 K. However, warming **5** to room temperature results in the immediate re-formation of **1a**.

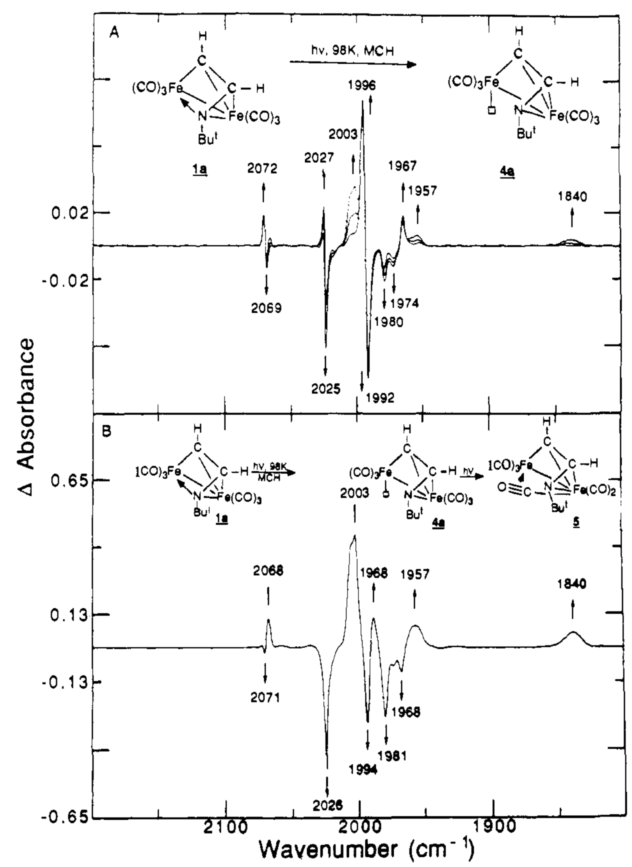

Figure 1. (A) IR spectral changes accompanying near-UV irradiation of 3.3 mM *tert*-butylferraazetine **1a** in MCH at 98 K. Negative peaks are due to consumption of **1a**, and positive peaks are due to the appearance of the intermediate **4a**. **4a** has absorptions at 2072, 2027, 1996, and 1967 cm^{-1}. Conversion is 8.6% based on consumption of starting material. (B) Further irradiation to 41% consumption of **1a** resulting in the dominance of intermediate **5**, with absorptions at 2068, 2005, 2003, 1988, 1957, and 1840 cm^{-1}.

If large quantities of compounds **4a** and **5** (>30%) are generated by irradiation of **1a** at 98 K, trace quantities of the CO insertion product **2a** and $Fe(CO)_5$ are observed upon warmup. At long irradiation times, CO appears in the matrix, presumably a result of CO loss, albeit inefficient. The nature of the CO loss product has not been established.

Photochemistry of *tert*-Butylferraazetine 1a in MCH Solution at Room Temperature and at 8 K in ^{12}CO and ^{13}CO Matrices. Similar to the previously reported formation of **2a** from the room-temperature photolysis of **1a** in ^{12}CO-saturated pentane,[1] near-UV irradiation of **1a** in ^{12}CO-saturated MCH also gives rapid and clean formation of compound **2a**, eq 1. Figure 2A shows IR spectral changes accompanying the room-temperature photolysis of **1a** in ^{12}CO-saturated MCH, while Figure 2b shows the spectral changes in the presence of ^{13}CO. Note that the position of the band assigned to the acyl carbonyl (1715 cm^{-1}) is the same in both parts a and b of Figure 2, whereas the terminal metal carbonyl region (2100–1900 cm^{-1}) shows changes indicative of ^{13}CO incorporation (Figure 2B). This indicates that the origin of the CO of the acyl ligand in **2a** is a CO ligand of **4a** and *not* exogenous CO.

Figure 3 shows IR spectral changes accompanying irradiation of **1a** in ^{12}CO and ^{13}CO matrices at 8 K. As in MCH at 98 K, the primary photoprocess at 8 K in a CO matrix is Fe–N bond cleavage to give **4a**. However, at 8 K compound **4a** does not revert

---

[3] Rest, A. J.; Sodeau, J. R. *J. Chem. Soc., Chem. Commun.* **1975**, 696.

[4] (a) Hepp, A. F.; Blaha, J. P.; Lewis, C.; Wrighton, M. S. *Organometallics* **1984**, *3*, 174. (b) Hooker, R. H.; Mahmoud, K. A.; Rest, A. J. *J. Chem. Soc., Chem. Commun.* **1983**, 1022.

[5] (a) Bentsen, J. G.; Wrighton, M. S. *J. Am. Chem. Soc.* **1987**, *109*, 4530. (b) Sheline, R. K.; Pitzer, K. S. *J. Am. Chem. Soc.* **1950**, *72*, 1107.

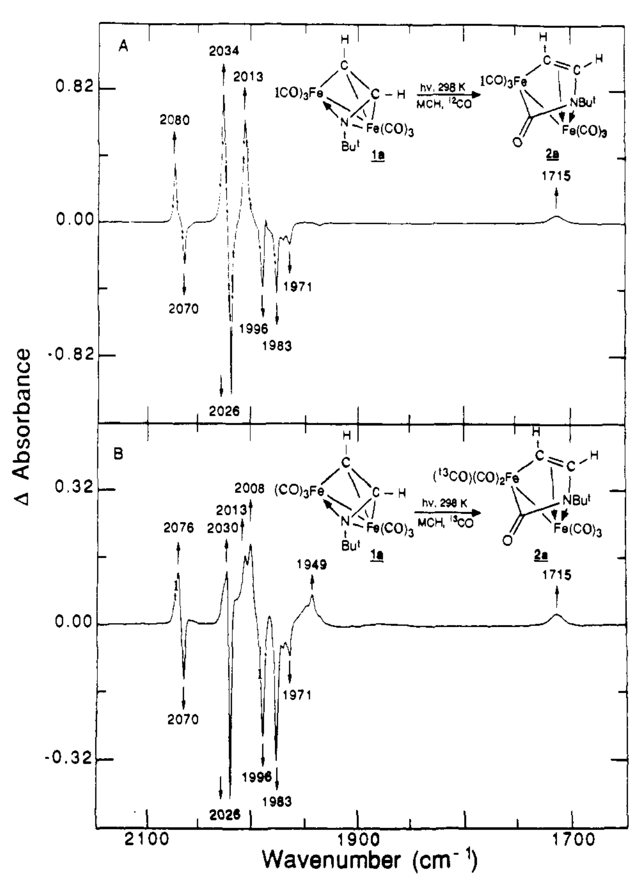

Figure 2. (A) IR spectral changes resulting from room-temperature irradiation of *tert*-butylferraazetine **1a** in ^{12}CO-saturated MCH. Negative peaks are due to consumption of **1a**, and positive peaks are due to the appearance of **2a**. **2a** has absorptions at 2080, 2034, 2013, 1994, 1982, and 1715 cm^{-1}. Absorptions at 1994 and 1982 cm^{-1} are obscured by loss of **1a**. (B) IR spectral changes resulting from room-temperature irradiation of *tert*-butylferraazetine **1a** in MCH saturated with ^{13}CO. Negative peaks are due to consumption of **1a** and positive peaks to the appearance of **2a**. Note that the CO absorptions in the terminal metal carbonyl region (2100–1900 cm^{-1}) are different than those appearing upon irradiation of **1a** in the presence of ^{12}CO (Figure 2A) but that the acyl CO appears in the same position, 1715 cm^{-1}.

Table I. IR Spectral Data for Relevant Compounds

complex	CO region of IR, cm^{-1} (ϵ, L/mol·cm)[a]
1a	2071 (3530), 2027 (13 400), 1996 (8780), 1984 (9070), 1971 (2060)
1b	2066 (4170), 2026 (13 800), 1994 (7350), 1981 (8590), 1970 (2620)
2a	2080 (5340), 2034 (12 200), 2013 (9930), 1994 (6920), 1982 (3940), 1715 (790)
2b	2076 (m), 2032 (s), 1715 (w)[b]
3a	2057 (5810), 2009 (14 700), 1983 (6900), 1972 (4730), 1957 (2780), 1952 (sh), 1618 (191)[c]
3b	2055 (7140), 2009 (12 100), 1984 (6020), 1972 (3360), 1956 (2120), 1952 (sh), 1618 (67)[c]

[a] IR data for MCH solutions at 293 K. [b] **2b** could not be isolated. [c] Imine stretch.

to **1a** in the dark. In a CO matrix, the secondary photoprocess results in insertion of CO between the Fe–C bond of the ferraazetine ring to give **2a**. Figure 3A shows IR spectral changes accompanying irradiation of **1a** at 8 K in ^{12}CO. Negative peaks are due to the consumption of **1a**, and the positive peaks at 2075, 2030, 2002, and 1967 cm^{-1} are due to the production of **4a**. Continued irradiation of **4a** produces bands at 2084, 2037, 2017, and 1708 cm^{-1} which are assigned to **2a** (Table I; differences in the position of the bands in Figure 3 as compared to the values given to the same compounds in Table I are due to differences in temperature and matrix composition). The most noticeable changes in the IR difference spectra of **1a** irradiated in a ^{13}CO matrix as compared to irradiation in a ^{12}CO matrix (Figure 3A,B) are the shifts in frequency for the bands in the terminal CO region and growth of a new band at 1952 cm^{-1}. Note that there is no indication of CO incorporation from the matrix into the acyl position of **2a**, indicating that the reactivity of **1a** at 8 K in a CO matrix parallels its reactivity at room temperature (i.e., the origin of the CO of the acyl ligand of **2a** is not exogenous CO).

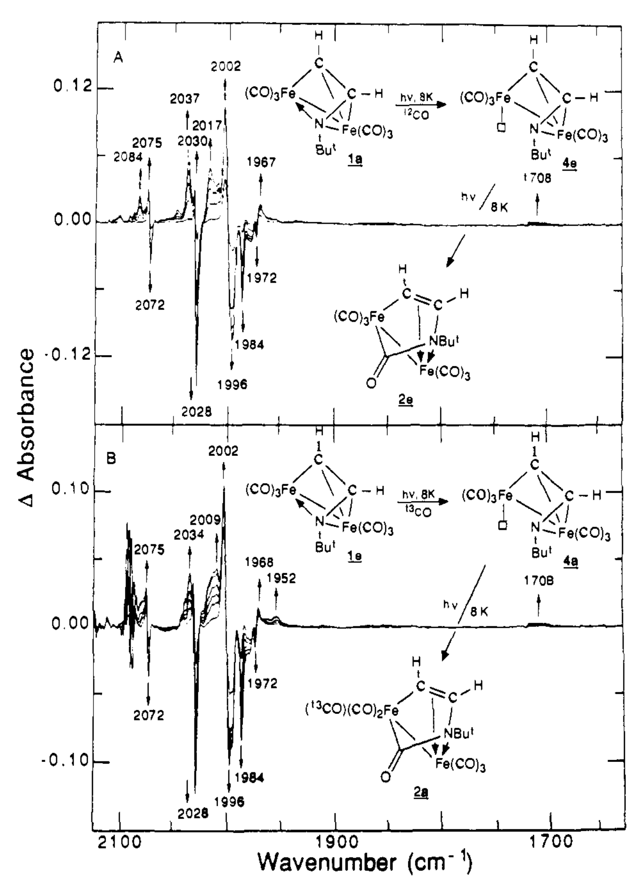

Figure 3. (A) IR spectral changes resulting from near-UV irradiation of *tert*-butylferraazetine **1a** in a ^{12}CO matrix at 8 K. Negative peaks are due to the consumption of **1a** and positive peaks to the appearance of first **4a** and then **2a**. (B) IR spectral changes resulting from irradiation of **1a** in a ^{13}CO matrix at 8 K. Negative peaks are due to the consumption of **1a** and positive peaks to the appearance of first **4a** and then **2a**. The region at $\nu > 2080$ cm^{-1} is obscurred due to matrix absorption. Note that in Figure 3B the CO absorptions in the terminal metal carbonyl region (2100–1900 cm^{-1}) are different for **2a** than those in Figure 3A (^{12}CO matrix) but that the acyl CO appears in the same position, 1708 cm^{-1}.

Photochemistry of *tert*-Butylferraazetine 1a at 98 K in a 1:1 MCH/*tert*-Butylacetylene Matrix. Near-UV irradiation of **1a** at 98 K in a rigid 1:1 MCH/*tert*-butylacetylene matrix results in initial Fe–N bond cleavage with the formation of **4a** (Figure 4A) consistent with results for a pure MCH matrix. At 98 K **4a** slowly reverts to **1a** in the dark. Further irradiation of **4a** in 1:1 MCH/*tert*-butylacetylene results in the formation of a new species which we propose to be the alkyne-coordinated compound **6** (Figure 4B). No free CO is detected in the matrix upon photolysis. Consistent with the proposed structure, the IR spectrum of **6**, unlike **5**, shows *no* bridging CO band, presumably because the *tert*-butylacetylene ligand occupies the vacant coordination site created by photoinduced N atom extrusion. Warming intermediate **6** to room temperature gives the expected *tert*-butylferrapyridine compound **3a** as the major product with a trace amount of $Fe(CO)_5$ and substantial regeneration of **1a** (>30%).

Temperature Dependence of *N*-*tert*-Butyl-2-styrylferraazetine 1b in MCH. Cooling a MCH solution containing ~3 mM $Fe_2(\mu\text{-}C(CH{=}CHPh)CHNBu^t)(CO)_6$ (**1b**) to form a rigid glass matrix results in the IR spectral changes illustrated in Figure 5. At 293 K in MCH, **1b** has IR absorption bands at 2066, 2026, 1994, 1981, and 1970 cm^{-1}. Upon cooling and formation of a glass,

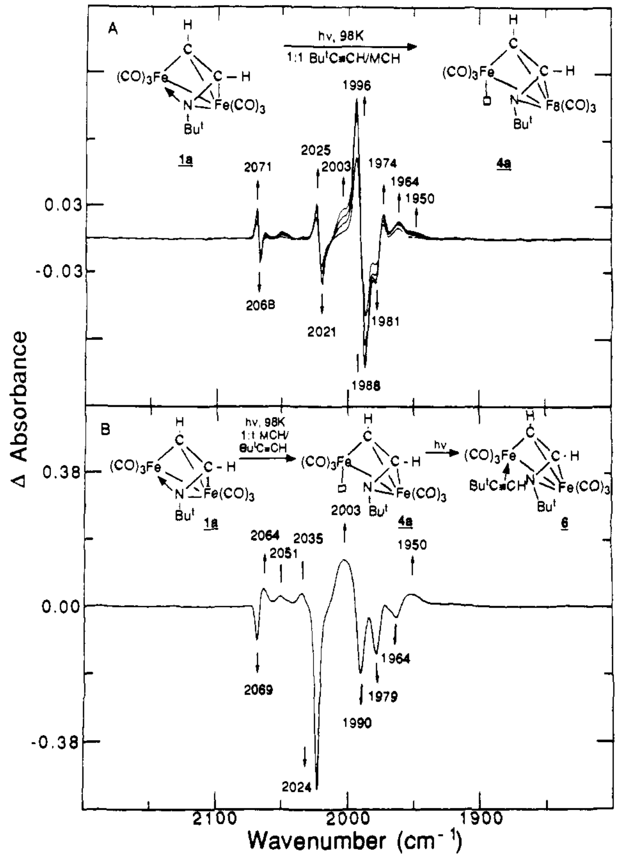

Figure 4. (A) IR spectral changes resulting from near-UV irradiation of 3.5 mM *tert*-butylferraazetine **1a** in a 1:1 MCH/*tert*-butylacetylene matrix at 98 K. Negative peaks are due to the consumption of **1a** and positive peaks to the appearance of **4a**. Conversion is 3.0% based on the consumption of starting material. (B) Further irradiation to 53% consumption of **1a** resulting in dominance of the alkyne-coordinated intermediate **6**, with absorptions at 2064, 2051, 2035, 2003, and 1950 cm^{-1}.

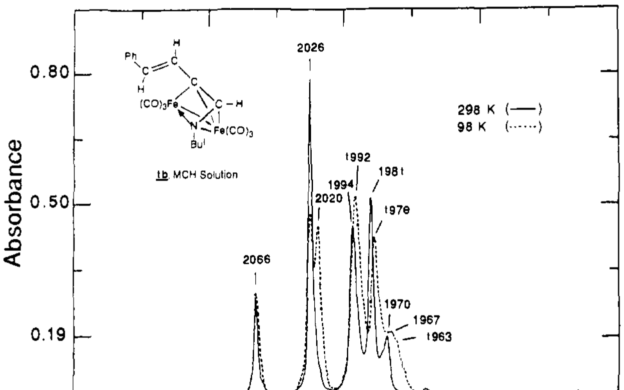

Figure 5. IR spectra of a ~3 mM solution of **1b** in MCH at 298 K (—) and at 98 K (···). At 298 K, absorptions appear at 2066, 2026, 1994, 1981, and 1970 cm^{-1}. At 98 K, absorptions appear at 2066, 2026, 2020, 1992, 1978, 1967, and 1963 cm^{-1} and relative intensities of bands appearing in the same position at each temperature have changed.

the sample exhibits a decrease in intensity for the band at 2026 cm^{-1} and the appearance of a new band at 2020 cm^{-1}. Subtle changes in intensity and position are also observed for the bands at 1994, 1981, and 1970 cm^{-1}. Under the same conditions, analogous spectral changes do not occur for **1a**.

Scheme I

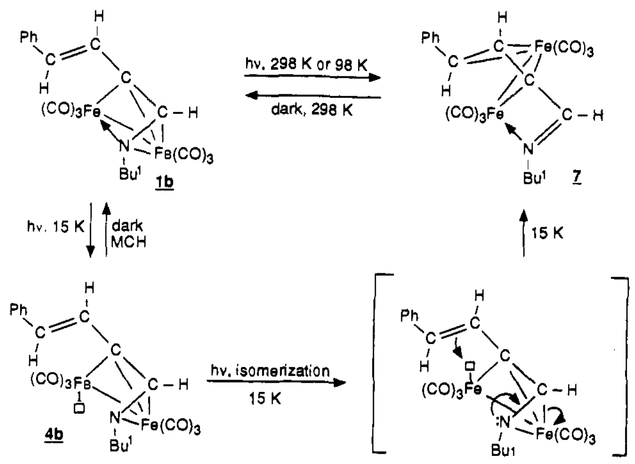

Chart I

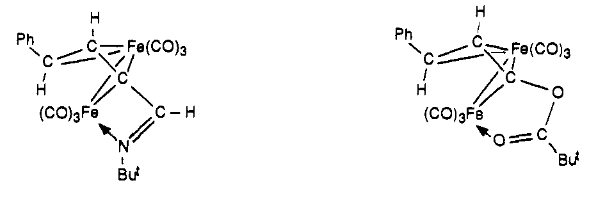

7

8

^{1}H NMR (CD$_2$Cl$_2$): δ 8.83 (s, $C\underline{H}NBu^t$)
δ 6.53 (d, J=9.5 Hz, $C\underline{H}CHPh$)
δ 3.81 (d, J=9.5 Hz, $C\underline{H}Ph$)

^{1}H NMR (CDCl$_3$): δ 6.67 (d, J=9.4 Hz, $C\underline{H}CHPh$)
δ 3.25 (d, J=9.4 Hz, $C\underline{H}Ph$)

The spectral changes occur only at the glass transition temperature of the MCH. Apparently, when the solution forms a glass, each molecule of **1b** is locked into one of several possible structural conformations associated with the rotational free pendant styryl group. The IR spectral changes can be reversed by warming the glass to 298 K.

Photochemistry of *N*-*tert*-Butyl-2-styrylferraazetine 1b at 298 K in MCH and at 98 K in a MCH Matrix. Irradiation of **1b** in MCH at 298 K results in rapid formation of a new species, **7** (Scheme I). Based upon FTIR, ^{1}H NMR, and ^{13}C NMR data, we propose the structure of **7** to be the π-bound ferrabutadiene complex shown in Scheme I. The ^{1}H NMR is consistent with the structure proposed for **7** and compares well with the ^{1}H NMR data for the similar π-bound ferrabutadiene complex **8** reported by Watanabe and co-workers[6] (Chart I). The photoinduced Fe(CO)$_3$ migration in Scheme I is similar to photoinduced haptotropic rearrangement observed for (C$_{11}$H$_{12}$)Fe(CO)$_3$ where an Fe(CO)$_3$ group migrates along the extended π-system of 2,2-dimethylindene ligand, eq 3.[7a] However, the mechanism for the two rearrangements are not necessarily related (see Discussion).

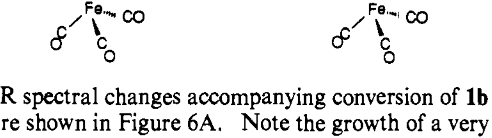

(3)

IR spectral changes accompanying conversion of **1b** to **7** at 298 K are shown in Figure 6A. Note the growth of a very weak band at 1592 cm^{-1}, which is presumably due to the transition-metal-free imine that **7** possesses and **1b** does not. Also, note that the three bands of **7** (2053, 2012, 1978 cm^{-1}) appear at lower frequencies than the three bands assigned to **1b** (2066, 2026, 1995 cm^{-1}), which is a consequence of replacing a weak σ-donating, η^2-bound imine ligand with a relatively strong σ-donating, η^2-bound styryl ligand at the Fe(CO)$_3$ center to which the ferraazetine ring is bound. Upon being allowed to stand in the dark for ~2 h, **7** quantitatively reverts to starting complex **1b**.

---

(6) Mitsudo, T.; Ishihara, A.; Kadokura, M.; Watanabe, Y. *Organometallics* **1986**, *5*, 238.

(7) (a) Zou, C.; Wrighton, M. S. *Organometallics*, in press. Another example of photoinduced haptotropic rearrangement: (b) Nagashima, H.; Fukahori, T.; Itoh, K. *J. Chem. Soc., Chem. Commun.* **1991**, 786.

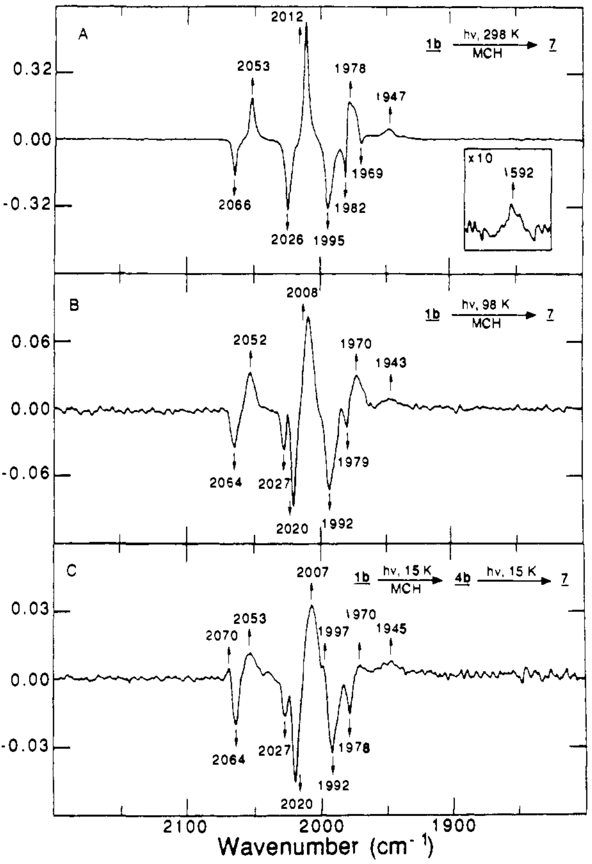

Figure 6. (A) IR spectral changes accompanying room-temperature irradiation of **1b** in MCH. Negative peaks are due to the consumption of **1b** and positive peaks to the appearance of **7**, which has absorptions at 2053, 2012, 1978, 1947, and 1592 cm^{-1}. Upon being allowed to stand in the dark at 298 K for 2 h, **7** quantitatively re-forms **1b**. (B) IR spectral changes accompanying 98 K irradiation of **1b** in MCH. Negative peaks are due to the consumption of **1b** and positive peaks to the appearance of **7**. Upon being warmed to room temperature, **7** quantitatively re-forms **1b** after 2 h. (C) IR spectral changes accompanying 15 K irradiation of **1b** in MCH. Negative peaks are due to the consumption of **1b**. Positive peaks at 2070 and 1997 cm^{-1} are due to the formation of **4b**.

The conversion from **7** back to **1b** in CD_2Cl_2 can be monitored by ^{1}H NMR (Figure 7). Illustrated in Figure 7 are five successive ^{1}H NMR spectra of a 3:2 mixture of photogenerated **7** and **1b** taken periodically as the same is allowed to stand in the dark at 298 K for 105 min. Over the 105-min time period, a gradual but constant decrease in intensity for the resonances assigned to **7** and growth of the resonances assigned to starting material **1b** may be observed.

Irradiation of 3 mM **1b** in a rigid MCH matrix at 98 K also results in the formation of **7** (Figure 6B). The reaction is *rapid* when compared to the photoinduced conversion of **1a** to **4a** and **5** at 98 K (Figure 1A,B). Like **1a**, dissociative loss of CO is not a primary photoprocess for **1b** as indicated by the lack of free CO in the matrix. At 98 K, intermediate **7** will not re-form starting material, but when warmed to room temperature, **7** will quantitatively re-form **1b** over a 2-h time period.

Near-UV irradiation of a MCH matrix containing **1b** at 15 K results in rapid conversion to a mixture of compounds containing a substantial amount of **7** and a new compound whose identity we assign to be **4b** (Figure 6C). We conclude that the new product formed at 15 K and not at 98 or 298 K is **4b** due to the bands observed at 2070 and 1997 cm^{-1} which are similar in frequency to those found for **4a** (Figures 1A and 4A). The bands at 2027 and 1967 cm^{-1} that are assigned to **4a** in Figures 1A and 4A would also be expected to be present for **4b**. However, these bands are obscured in Figure 6C because of overlap with bands due to the consumption of **1b** and production of **7**. At 15 K in the dark, **4b** re-forms **1b**. The fact that **4b** can be spectroscopically observed at 15 K but not at 98 K suggests that the conversion of **4b** to **7** is a thermal process which proceeds at 98 K but not at 15 K (Scheme I). However, continued photolysis of **4b** at 15 K leads to production of **7**, indicating that **7** can be formed photochemically as well as thermally. The relative importance of the thermal and photochemical processes depends on temperature and light intensity. This explains why the 98 K photochemically induced transformation of **1b** to **7** proceeds at a much faster rate than the analogous photoinitiated transformation of **1a** into **5** at the same temperature and light intensity. Both processes involve initial formation of **4**, but at 98 K **4b** can thermally form **7** whereas **4a** needs an additional photon to form **5**.

Photochemistry of *N*-*tert*-Butyl-2-styrylferraazetine 1b at 298 K in ^{12}CO-, ^{13}CO-, and *tert*-Butylacetylene-Saturated MCH. Near-UV irradiation of **1b** at 298 K in ^{12}CO-saturated MCH yields product **7** (conversion ~38%) with no apparent formation of CO insertion product $Fe_2\{\mu\text{-}C(CH{=}CHPh)CHNBu^tC(O)\}(CO)_6$ (**2b**). However, upon being allowed to stand in the dark for 1 h, **7** proceeds to form the CO insertion product **2b**, in addition to substantial amounts of starting material **1b**, eq 4. **2b** is also formed if **7** is generated in the absence of CO, and CO is then introduced in the dark. Clearly, in the case of **1b**, CO insertion is a result of thermal CO reaction with **7**. *tert*-Butylacetylene when added in the dark to a MCH solution of photogenerated **7** gives the expected ferrapyridine product **3b** (conversion ~3%) in addition to starting material **1b**, eq 5.

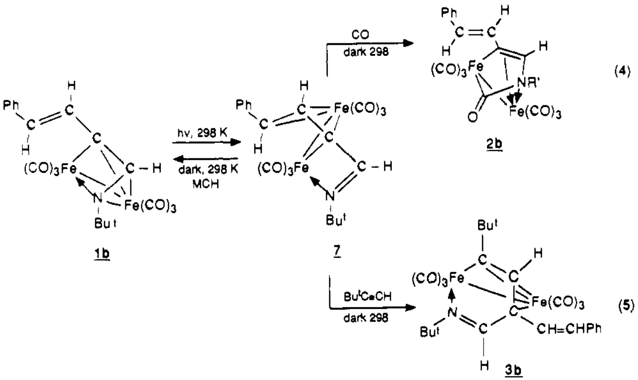

Figure 8A shows the IR spectral changes accompanying thermal reaction of **7** with ^{12}CO at 298 K to give **2b** (and regeneration of **1b**). Compound **2b** has IR absorptions that are almost identical to those of **2a** (Table I). Addition of ^{13}CO to a MCH solution containing **7** results in the formation of the CO-insertion product **2b** with ^{13}CO incorporation occurring exclusively at a terminal position (Figure 8B). Note that the position of the acyl band is the same in parts A and B of Figure 8 indicative of ^{12}CO incorporation at that site. However, the absorbances in the terminal CO region (2100–1900 cm^{-1}) in Figure 8A,B differ, indicating ^{13}CO incorporation at one of the terminal carbonyl sites of **2b**.

Discussion

Illustrated in Scheme II are the proposed low-temperature photoprocesses for compound **1a** in the absence and presence of *tert*-butylacetylene and CO. In all three cases, compound **1a** undergoes initial light-induced Fe–N bond cleavage to yield compound **4a**. This process is thermally reversible at 98 K but not at 8 K. In the absence of *tert*-butylacetylene, near-UV irradiation of **4a** produces the bridging CO compound **5**. Irradiation of **4a** in a 1:1 *tert*-butylacetylene/MCH matrix yields alkyne-coordinated complex **6**. Neither **5** nor **6** will revert to **4a** at 98 K, but warming **5** to 298 K in MCH results in regeneration of **1a** and warming **6** to 298 K produces ferrapyridine compound **3a**. Irradiation of **4a** in a CO matrix gives CO insertion product **2a**, and when the matrix is ^{13}CO, ^{13}CO incorporation is found at a terminal Fe–CO position and not at the carbonyl of the acyl site of **2a**.

Typically, there are two possible and often times competing processes in the photochemistry of binuclear organometallic carbonyl complexes: photoinduced ligand dissociation and met-

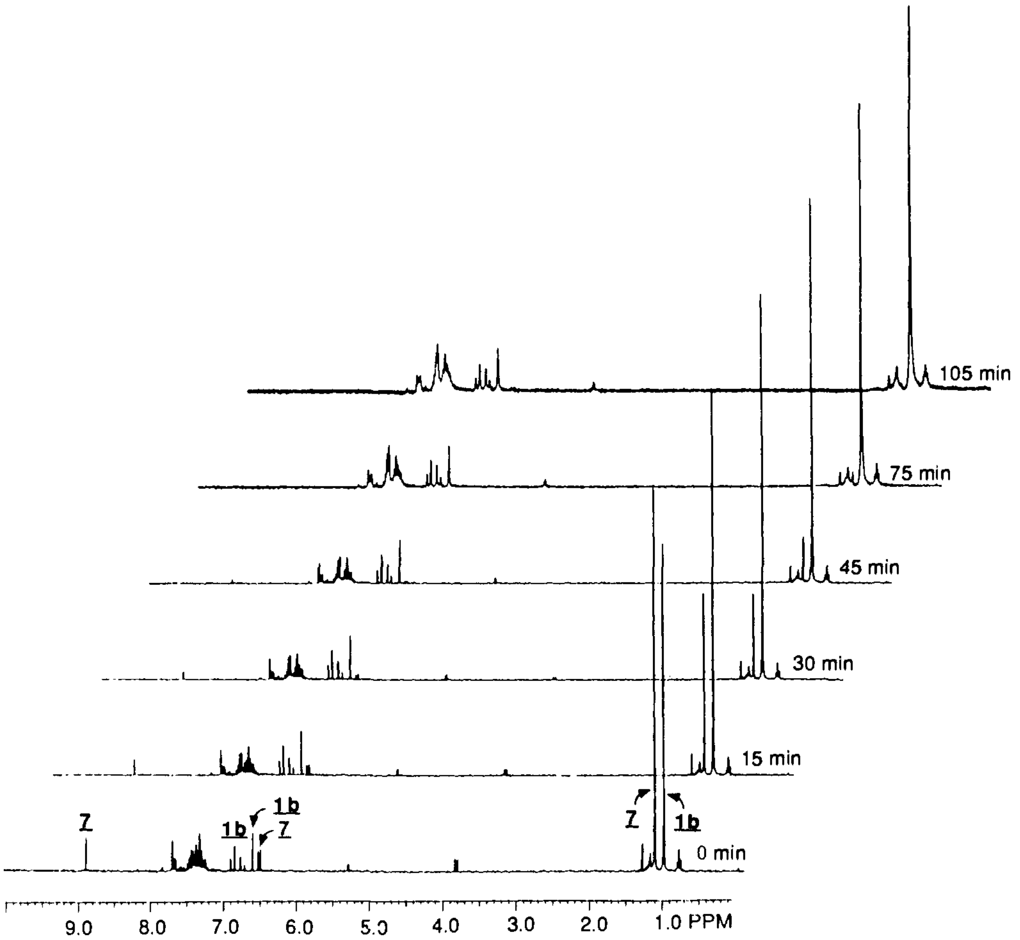

Figure 7. ^{1}H NMR spectral changes accompanying the thermal conversion of photogenerated **7** to **1b** at 298 K in CD_2Cl_2 solution.

Scheme II

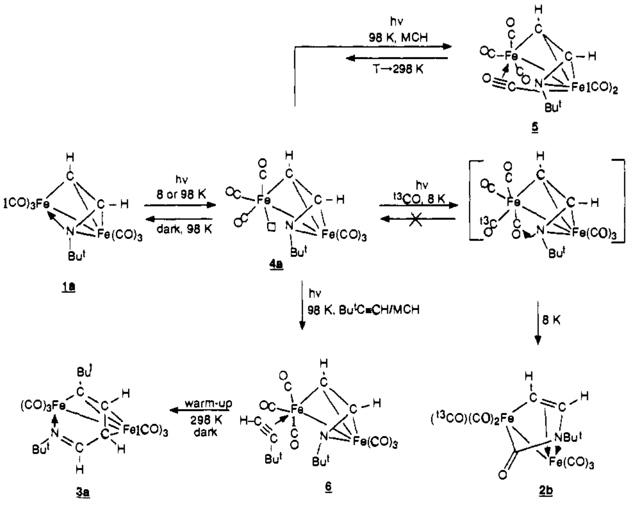

al–metal bond breakage.[8] The conversion of **1a** to **4a** is an example of a photoinduced ligand dissociation reaction involving loss of a N-donor ligand. The second photoprocess, which involves conversion of **4a** to **5**, **6**, or **2a**, is more ambiguous. It is interesting that the second photoprocess is necessary for ligands such as CO or *tert*-butylacetylene to coordinate to electronically unsaturated **4a**. But perhaps even more interesting is the necessary absorption of a second photon in the conversion of **4a** to bridging carbonyl compound **5** (Scheme II). There are several examples of photoinduced ligand dissociation from binuclear transition-metal carbonyl compounds to form complexes with bridging CO ligands,[4,9] but for these examples, the bridging process is an immediate consequence of photoinduced CO dissociation from one of the metal centers. This seems to suggest that the vacant coordination site in **4a** is not accessible to coordinating ligands such as *tert*-butylacetylene or CO even when they are the major components of a matrix. In fact, **4a** contains a vacant site that is inaccessible to even its own CO ligands as evidenced by its inability to form bridging carbonyl compound **5** in the dark. We therefore propose that the second photoprocess in the transformation of **4a** to **5**, **6**, and **2a** is an isomerization of **4a** that moves the vacant coordination site to a position more accessible to incoming ligands (i.e., away from the N atom).

Photoisomerizations for groups VI and VII mononuclear transition-metal carbonyl complexes are well precedented.[10] For example, the coordinatively unsaturated C_{4v} and C_s isomers of $(CH_3)Re(CO)_4$ may be photochemically interconverted through a photoinduced CO ligand migration,[10a] eq 6. Similarly, **4a** could undergo a photoinduced CO migration which would move one of its CO ligands to the site originally occupied by the N atom, eq 7. The vacant coordination site of **4a** would then be in a position

---

(8) (a) Geoffroy, G. L.; Wrighton, M. S. *Organometallic Photochemistry*; Academic Press: New York, 1979. (b) Meyer, T. J.; Caspar, J. V. *Chem. Rev.* **1985**, *85*, 187–218. (c) Bursten, B. E.; McKee, S. D. *J. Am. Chem. Soc.* **1991**, *113*, 1210 and references therein.

(9) (a) Firth, S.; Hodges, P. M.; Poliakoff, M.; Turner, J. J. *Inorg. Chem.* **1986**, *25*, 4608. (b) Pope, K. R.; Wrighton, M. S. *Inorg. Chem.* **1987**, *26*, 2321. (c) Hepp, A. F.; Wrighton, M. S. *J. Am. Chem. Soc.* **1983**, *105*, 5934. (d) Dunkin, I. R.; Härter, P.; Shields, C. J. *J. Am. Chem. Soc.* **1984**, *106*, 7248.

(10) (a) Firth, S.; Horton-Mastin, A.; Poliakoff, M.; Turner, J. J.; McKean, D. C.; McQuillan, G. P.; Robertson, J. *Organometallics* **1989**, *8*, 2876, and references therein. (b) Church, S. P.; Poliakoff, M.; Timney, J. A.; Turner, J. J. *Inorg. Chem.* **1983**, *22*, 3259. (c) Poliakoff, M. *Inorg. Chem.* **1976**, *15*, 2892. (b) Black, J. D.; Braterman, P. S. *J. Organomet. Chem.* **1973**, *63*, C19.

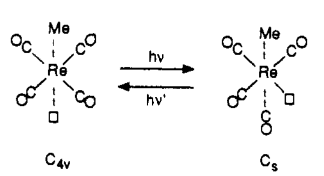

(6)

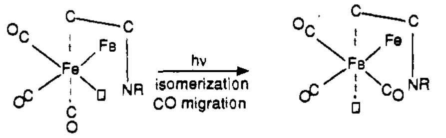

4a

(7)

that is more accessible to incoming ligands. In eq 6 it is clear that as the reaction proceeds from left to right, a CO cis to the CH_3 group moves to a trans position. However, the lack of symmetry in **4a** precludes the possibility of predicting which CO may be migrating, eq 7. Although CO migration is consistent with the observed results, we cannot rule out photoinduced $Fe(CO)_3$ rotation as a possible isomerization pathway. Bergman has proposed CpCo rotation in the thermal cis/trans isomerization of $[CpCoCO]_2(\mu\text{-}CH_2)$.[11]

In Scheme II the incoming ligand (*tert*-butylacetylene or CO) fills the vacant coordination site of photoisomerized **4a**. The addition of CO appears to activate the complex and to render one of its CO ligands susceptibile to nucleophilic attack by the N atom. In contrast, the *tert*-butylacetylene ligand of **6** and the bridging CO ligand of **5** do not affect **4a** in the same manner (Scheme II), and N atom attack at a CO ligand in complexes **5** and **6** does not occur. This can be spectroscopically verified by the absence of acyl bands in the IR spectra for compounds **5** and **6**. It is understandable that the addition of CO to **4a** increases the electrophilicity of its CO ligands whereas alkyne coordination does not. Angelici and others have shown that an overall decrease in metal to ligand back-bonding for transition-metal carbonyl complexes increases the susceptibility of these complexes to nucleophilic attack.[12] CO is a better π-acceptor than *tert*-butylacetylene, and *tert*-butylacetylene is a better σ-donor than CO. Therefore, CO coordination to **4a**, when compared with *tert*-butylacetylene coordination, yields a relatively less electron-rich Fe center. The net effect is that in the case of CO coordination the CO ligands of **4a** are made susceptible to nucleophilic attack whereas in the cases of *tert*-butylacetylene coordination to **4a** and CO bridging within **4a** the CO ligands are not made susceptible to nucleophilic attack by the N atom (Scheme II).

The strongest evidence for the second photoprocess involving **4a** isomerization comes from the comparison of the results obtained with ^{13}CO and ^{12}CO matrices. If isomerization did not occur, photoinduced Fe–N bond cleavage in **1a** followed by CO coordination and subsequent N atom attack would yield **2a** with an acyl carbonyl that came from exogenous CO. If this were the case, reaction in a ^{13}CO matrix would yield **2a** with ^{13}C incorporation at the acyl position. However, ^{13}C incorporation at room temperature and at 8 K does not occur in the acyl position but instead occurs at a terminal position in **2a**, indicating that Fe–N bond cleavage followed by ligand coordination to a geometrically unperturbed $Fe(CO)_3$ center is not occurring. Instead, photoisomerization of **4a** must occur so that the vacant coordination site becomes accessible to incoming ligands such as CO and *tert*-butylacetylene.

The photoisomerization of intermediate **4a** is required for reaction with incoming ligands and explains why CO insertion occurs between the Fe–N bond of the metallacycle whereas alkyne insertion does not. When the alkyne coordinates to **4a** to form **6**, the coordination site it occupies is no longer near the N atom, eq 7. Therefore, the N atom of **6** cannot attack the alkyne ligand, so the insertion of the alkyne between the Fe–C bond of the ferraazetine ring to yield **3a** appears to be the favored pathway (Scheme II).

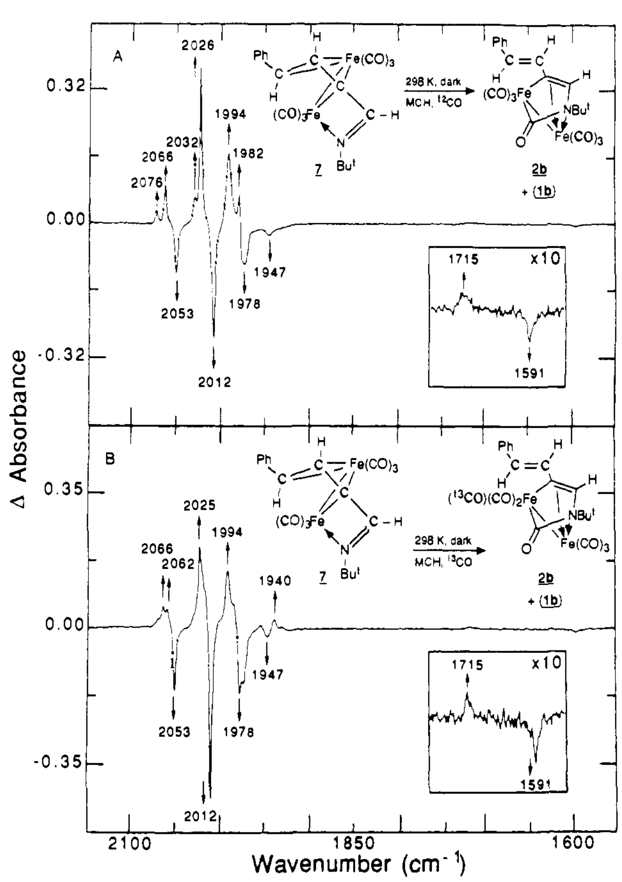

Figure 8. (A) IR spectral changes accompanying thermal reaction of photogenerated 7 with ^{12}CO. Negative bands are due to the consumption of 7 and positive peaks to the appearance of **2b** and **1b**. Absorptions at 2076, 2032, and 1715 cm^{-1} are assigned to **2b** based on their similarity to those of **2a** (Table I). Absorptions at 2066 and 2026 cm^{-1} are due to **1b**, and those at 1994 and 1982 cm^{-1} are due to both **2b** and **1b**. (B) IR spectral changes accompanying thermal reaction of photogenerated 7 with ^{13}CO. Negative peaks are due to the consumption of 7 and positive peaks to the appearance of **2b** and **1b**. Note that the CO absorptions in the terminal metal carbonyl region (2100–1900 cm^{-1}) are different from those appearing upon thermal reaction of 7 with ^{12}CO (Figure 8A) but that the acyl CO appears in the same position (1715 cm^{-1}).

The photochemistry of **1b** is consistent with that of **1a**. Although the photoisomerization of **1b** to **7** would appear to involve migration of the π-bound $Fe(CO)_3$ group from the imine portion of the ferraazetine metallacycle to the pendant styryl ligand, the transformation most likely occurs through a ligand substitution reaction of the pendant styryl group for the N atom of **1b** (Scheme I). This chemistry is consistent with the conclusion that the primary photoprocess in **1a** and **1b** specifically involves dissociation of the dative-bound N atom of the ferraazetine ring from the Fe center that is part of the metallacycle. For **1a** and **1b**, it is unlikely that any of the primary photoprocesses involve extrusion of the imine group from π-bound $Fe(CO)_3$, since the FTIR spectra for intermediates **4a**, **4b**, **5**, and **6** do not exhibit bands characteristic of a free imine.[13]

Compound **7**, like **5** and **6**, is another trapped form of isomerized intermediate **4**, and accordingly, **7** reacts with CO and *tert*-butylacetylene to yield insertion products **2b** and **3b**, eqs 4 and 5, respectively. In fact, reaction of **7** with ^{13}CO yields **2b** with ^{13}CO incorporation at a terminal Fe–CO position and not at the carbonyl

---

(11) Theopold, K. H.; Bergman, R. G. *J. Am. Chem. Soc.* **1983**, *105*, 464–475.

(12) (a) Bush, R. C.; Angelici, R. B. *J. Am. Chem. Soc.* **1986**, *108*, 2735. (b) Angelici, R. *Acc. Chem. Res.* **1972**, *5*, 335. (c) Darensbourg, D. J.; Darensbourg, M. Y. *Inorg. Chem.* **1970**, *9*, 1691. (d) Angelici, R. J.; Christian, P. A.; Dombek, B. D.; Pfefer, G. A. *J. Organomet. Chem.* **1974**, *67*, 287.

(13) Vogel, A. *Vogel's Textbook of Practical Organic Chemistry*, 4th ed.; Longman: London, 1978; Chapter 7.

of the acyl ligand suggesting that exogenous CO is filling the coordination site held by the styryl ligand. The decreased rate of reaction between **7** and *tert*-butylacetylene or CO when compared to that for the reaction between **4a** and these ligands is due to the fact that *tert*-butylacetylene and CO must displace the styryl ligand of **7** before they can react to form insertion products **2b** and **3b**.

In conclusion, the work herein has demonstrated that (1) the conversion of *tert*-butylferraazetine **1a** to its CO and alkyne insertion products is not a simple one-photon process but rather a complicated two-photon process (at 98 K) that involves initial N atom extrusion from the Fe center that is part of the ferraazetine followed by an isomerization of the coordinatively unsaturated intermediate, (2) the isomerization of intermediate **4** can be thermal as well as photochemical depending on the temperature of the matrix/solution and the nature of the pendant groups, and (3) alkyne coordination to the metal center occurs prior to alkyne insertion and insertion occurs at a different position in the ferraazetine ring than does CO insertion because of the photoisomerization.

Experimental Section

Instruments and Equipment. IR spectra were recorded using a Nicolet 60SX, 740, or 170SX Fourier transform infrared spectrometer (resolution 2 cm^{-1}). ^{1}H NMR were recorded using a Bruker WM250 Fourier transform spectrometer. IR spectra were recorded in deoxygenated alkane solutions, held in 0.2-mm path length NaCl or CaF_2 cells. All MCH matrices were doped with 2% 3-methylpentane to prevent cracking. IR measurements at 98 K in MCH were performed with a Precision Cell, Inc., Model P/N 21000 variable-temperature cell with CaF_2 inner and outer windows, using N_2 as the coolant. The temperature of the cell was measured using a Cu–constantan thermocouple in contact with the inner window of the cell. Experiments at 15 K were performed using a CTI Cryogenic spectrum sample conditioner with CaF_2 inner and outer windows. Experiments at 8 K were carried out with the use of a CTI Cryogenics Model 2 Helix refrigerator, using a CsI window for gas matrix deposition in a shroud with KBr windows. Irradiations were effected with either a Baush and Lomb SP200 high-pressure Hg lamp filtered by a 10-cm H_2O filter with quartz windows or a Hanovia medium-pressure Hg lamp with a H_2O/quartz cooling jacket. Preparatory scale irradiations were carried out in Pyrex flasks, and the reactions proceeded identically to those in CaF_2 or NaCl cells. Standard Schlenk techniques in combination with the use of a Vacuum Atmospheres Co. drybox were used in the preparation of materials.

Solutions of **1a** and **1b** were prepared by dissolving the appropriate complex in MCH such that the absorbance of the most intense IR peak did not exceed 1.0 (solution concentrations may be calculated from the extinction coefficients for **1a** and **1b**; see Table I). The lineshape of the IR spectrum for **1a** at 298 K in MCH is almost identical to that of **1b** under the same conditions (Figure 5). Upon cooling of **1a** in MCH to 98 K, the spectrum shifts slightly to lower frequency but retains pattern integrity, unlike that of **1b** at 98 K (Figure 5). Cooling MCH solutions (>4.0 mM) of **1a** and **1b** to 98 K led to aggregation and significantly broadened IR bands. When aggregation was observed, fresh solutions of **1a** or **1b** at lower concentrations were prepared, and if there were no signs of aggregation, the appropriate experiment was performed.

Materials. MCH and 3-methylpentane were purchased from Aldrich Chemical Co. and were distilled from sodium under Ar and stored over molecular sieves prior to use. *tert*-Butylacetylene was used as received from Aldrich. CO, CP Grade, was purchased from Linde Specialty Gases. ^{13}CO was purchased from Cambridge Isotope Laboratories or from Stohler Isotope Chemicals. Compounds **1a**,[1] **1b**,[2b] **2a**,[1] and **3a**[2] were prepared by literature methods.

Conversion of *tert*-Butylferraazetine 1a to *tert*-Butylferrapyrrolinone 2a in MCH. The procedure used to convert **1a** to **2a** in MCH was similar to that reported in pentane.[1] In a typical reaction, ~2 mL of a 3 mM solution of **1a** was placed in a Pyrex test tube under Ar and sealed with a septum. The orange solution was purged with CO and irradiated. After ~2-min photolysis, the solution turned red and IR analysis (see Table I) indicated that conversion of **1a** to **2a** had taken place (78%). The transformation could be reversed by purging the solution with Ar for five min and stirring in the dark for ~24 h at room temperature.

Synthesis of Ferrapyridine Complex 3b from *tert*-Butylacetylene and 1b. Complex **1b** (0.13 mmol) was placed in a 100-mL Schlenk flask to which were added CH_2Cl_2 (60 mL) and 1.1 equiv of *tert*-butylacetylene. Stirring was commenced, and the resulting orange solution was irradiated for 4.5 h. The color changed to dark red, and the IR spectrum of the resulting solution showed disappearance of bands due to **1b** and appearance of a new set of bands assigned to **3b**. The solvent was removed by rotary evaporation, and the resulting residue was chromatographed on silica gel with pentane as the eluant to give a single orange band which was determined to be **3b** (0.095 mmol, yield 73%). **3b** could also be formed by the addition 1 equiv of *tert*-butylacetylene in the dark to photogenerated **7** (described above). The yield was substantially lower (~3% as determined by IR) using this method.

3b: Anal. Calcd for $C_{26}H_{27}Fe_2NO_6$: C, 55.65; H, 4.85. Found: C, 55.79; H, 5.15. MS: *m/z* 505 ($M^+ - 2$ CO) and fragment ions corresponding to the loss of four carbonyls. ^{1}H NMR (C_6D_6): δ 8.12 (s, 1 H), 8.12 (s, 1 H, C*H*=NH); 7.28–7.24 (m, 3 H, Ph); 7.11–7.05 (m, 2 H, Ph); 6.60 (d, 1 H, $J = 16.2$ Hz, C*H*); 6.48 (d, 1 H, $J = 16.2$ Hz, C*H*); 5.86 (s, 1 H, Bu^{t}CC*H*); 1.65 (s, 9 H, $NC(CH_3)_3$); 0.81 (s, 9 H, $CC(CH_3)_3$). ^{13}C NMR ($CDCl_3$): δ 214.0, 211.7, 209.9 (*C*O); 202.6 (s, *C*Bu^t); 177.5 (d, *C*H=N, $^1J_{CH} = 161.7$ Hz); 137.2 (s, Ph-ipso); 135.9 (d, *C*H, $^1J_{CH} = 153.8$ Hz); 128.8, 127.4, 125.8 (Ph); 126.2 (d, *C*H, $^1J_{CH} = 147.3$); 90.6 (d, Bu^{t}C*C*H, $^1J_{CH} = 163.3$ Hz); 64.6 (m, $C(CH_3)_3$); 63.8 (m, $C(CH_3)_3$); 45.4 (s, *C*CH=CHPh); 35.2 (m, $C(CH_3)_3$); 31.7 (m, $C(CH_3)_3$).

Photoconversion of *N*-*tert*-Butyl-2-styrylferraazetine 1b to Product 7. In a typical reaction, 2 mL of an orange 3 mM MCH solution of **1b** was placed in a Pyrex test tube which was sealed with a septum and deoxygenated via an Ar purge. Photolysis for 5 min resulted in a deep red solution of **7**, 38% conversion as determined by IR. Upon being allowed to stand in the dark for 2 h at room temperature, compound **7** quantitatively re-formed compound **1b**.

Synthesis of *N*-*tert*-Butyl-2-styrylferrapyrrolinone Complex 2b. Photoconversion of **1b** to **7** was achieved as previously described with the exception that the solution was purged with CO for 2 min prior to and during irradiation. Initially, clean conversion of **1b** to **7** (38% based on loss of **1b**) was observed by IR with no detectable formation of **2b**. When the solution was allowed to stir in the dark for 1 h under CO, the IR bands assigned to **7** disappeared and those assigned to **1b** reappeared along with new bands which were assigned to **2b** (see Table I). After the mixture was allowed to stand in the dark for an additional 4 h, CO deinsertion from **2b** to form **1b** had occurred. Compound **2b** proved to be too reactive to isolate and was characterized on the basis of its similiratity to **2a** with respect to its IR spectrum.

Photoconversion of 1b to 2b with ^{13}CO. A 3 mM solution of **1b** in MCH was prepared in a test tube and converted to **7** (38% conversion) as described above. The mixture was freeze–pump–thaw degassed three times and then placed under 1 atm of ^{13}CO. The solution was stirred in the dark, and the reaction was monitored by FTIR. After 1 h, predominant re-formation of **1b** had occurred in addition to formation of a small amount of **2b**. ^{13}CO incorporation occurred at a terminal position in **2b** as evidenced by shifts in the bands between 2100 and 1900 cm^{-1}. The acyl band remained at the ^{12}CO frequency of 1715 cm^{-1} (Figure 8B).

Low-Temperature Matrix Photochemistry of 1a and 1b. In a typical reaction, a 3 mM MCH solution of **1a** or **1b** was loaded into a 0.2-mm path length CaF_2 cell in an Ar drybox and placed in the low-temperature apparatus described above. After being cooled to 98 K, the sample was irradiated and changes in the IR region between 2200 and 1500 cm^{-1} as a function of irradiation time were recorded. In the case of **1a**, photoconversion to **4a** and **5** is slow, with only 25% conversion to the former occurring after ~5 min of irradiation. In the case of **1b**, photoconversion to **7** is rapid with 25% conversion occurring after 30 s of photolysis.

Photochemistry in Gas Matrices at 8 K. In a typical reaction the CsI window in the apparatus described above was cooled to 30 K under vacuum. At this point, a valve was opened between a deposition port and an evacuated flask cooled to 0 °C containing 3 mg of the compound to be studied. Along with a slow stream of the gas to be used as a matrix, the sample was deposited over a 2-h time period and then cooled to 8 K for irradiation and FTIR analysis.

Acknowledgment. This material is based on work supported by the National Science Foundation under Grant CHE-9002006 awarded in 1990 to C.A.M. in the form of an NSF Postdoctoral Research Fellowship and in part on grant support to M.S.W. from NSF and grant support to G.L.G. from the Office of Basic Energy Sciences, Department of Energy. We thank Professor Robert J. McMahon and Terry Barnhart at the University of Wisconsin at Madison for technical assistance and for allowing us to use their low-temperature matrix deposition apparatus for the experiments performed at 8 K.

Registry No. 1a, 125641-66-9; **1b**, 138053-61-9; **2a**, 122539-44-0; **2b**, 138653-62-0; **3a**, 125641-62-5; **3b**, 138053-63-1; **4a**, 138053-64-2; **4b**, 138053-65-3; **5**, 138089-49-3; **6**, 138053-66-4; **7**, 138053-67-5; Bu^{t}C≡CH, 917-92-0.